

# In Search for Optimal Targets for Intraoperative Fluorescence Imaging of Peritoneal Metastasis From Colorectal Cancer

Biomarkers in Cancer  
Volume 9: 1–7  
© The Author(s) 2017  
Reprints and permissions:  
sagepub.co.uk/journalsPermissions.nav  
DOI: 10.1177/1179299X17728254



Charlotte ES Hoogstins<sup>1</sup>, Benjamin Weixler<sup>1</sup>,  
Leonora SF Boogerd<sup>1</sup>, Diederik J Hoppener<sup>1</sup>, Hendrica AJM Prevoo<sup>1</sup>,  
Cornelis FM Sier<sup>1</sup>, Jacobus WA Burger<sup>2</sup>, Cornelis Verhoef<sup>2</sup>,  
Shadvhi Bhairosingh<sup>1</sup>, Arantza Farina Sarasqueta<sup>3</sup>,  
Jacobus Burggraaf<sup>4</sup> and Alexander L Vahrmeijer<sup>1</sup>

<sup>1</sup>Department of Surgery, Leiden University Medical Center, Leiden, The Netherlands.

<sup>2</sup>Department of Surgical Oncology, Erasmus MC Cancer Institute, Rotterdam, The Netherlands.

<sup>3</sup>Department of Pathology, Leiden University Hospital, Leiden, The Netherlands.

<sup>4</sup>Department of Pharmacology, Centre for Human Drug Research, Leiden, The Netherlands.

**ABSTRACT:** Peritoneal metastasis (PM) occurs in about 10% of patients with colorectal cancer (CRC). Fluorescence imaging can enhance contrast between cancerous and benign tissue, enabling the surgeon to clearly visualize PM during cytoreductive surgery. This study assessed the suitability of different biomarkers as potential targets for tumor-targeted imaging of PM of CRC. Tissue samples from primary tumor and PM from patients with CRC were obtained from the pathology archives and immunohistochemical stainings were performed. Overexpression of the epithelial cell adhesion molecule (EpCAM) and carcinoembryonic antigen (CEA) was seen in 100% of PM samples and the expression was strong in >70% of samples. Tyrosine-kinase Met (C-Met) and folate receptor  $\alpha$  overexpression was seen in 20% of PM samples. For successful application of tumor-targeted intraoperative fluorescence imaging of PM, biomarkers need to be identified. We demonstrated that both EpCAM and CEA are suitable targets for fluorescence imaging of PM in patients with CRC.

**KEYWORDS:** Image-guided surgery, fluorescence, colorectal cancer, peritoneal metastasis, metastasis, biomarkers

**RECEIVED:** May 22, 2016. **ACCEPTED:** July 14, 2017.

**PEER REVIEW:** Five peer reviewers contributed to the peer review report. Reviewers' reports totaled 903 words, excluding any confidential comments to the academic editor.

**TYPE:** Original Research

**FUNDING:** The author(s) received no financial support for the research, authorship, and/or publication of this article.

**DECLARATION OF CONFLICTING INTERESTS:** The author(s) declared no potential conflicts of interest with respect to the research, authorship, and/or publication of this article.

**CORRESPONDING AUTHOR:** Alexander L Vahrmeijer, Department of Surgery, Leiden University Medical Center, Albinusdreef 2, 2333 ZA Leiden, The Netherlands.  
Email: a.l.vahrmeijer@lumc.nl

## Introduction

Peritoneal metastasis (PM) is frequently seen in patients with colorectal cancer (CRC). Approximately 5% of patients already have PM at the time of diagnosis and another 5% will develop PM during the course of the disease.<sup>1</sup> Until the 1990s, PM was considered incurable and treatment consisted of palliative chemotherapy only. In 1993, Sugarbaker revolutionized the management of PM with the introduction of cytoreductive surgery (CRS) followed by hyperthermic intraperitoneal chemotherapy (HIPEC).<sup>2</sup> During CRS, all macroscopic tumor lesions are removed from the peritoneal cavity. Hereafter, a high dose of heated chemotherapy is administered intraperitoneally, hereby maximizing the local effect, whereas systemic exposure is kept to a minimum. Preoperative imaging modalities, including CT, have limited value in the detection of PM.<sup>3,4</sup> Due to the small size and superficial nature of PM lesions, extent of the disease is often underestimated by these modalities.<sup>3,4</sup> As a result, surgical exploration of the abdomen is performed prior to CRS, and the peritoneal cancer index (PCI) is assessed during the exploration.

Although morbidity (36%) and mortality (8%) associated with this aggressive treatment is high, patients undergoing CRS and HIPEC have a significantly improved overall

survival (22.3 months) compared with patients undergoing standard treatment consisting of only palliative chemotherapy (12.6 months).<sup>5–7</sup> Survival benefits decrease when a high number of abdominal regions (6 or 7) are affected by PM and when the PCI is >17.<sup>5–7</sup> Therefore, accurate assessment of the extent of the disease and careful patient selection are of utmost importance. Another prognostic predictor is the completeness of CRS, and survival percentage is higher in patients with a macroscopic complete resection compared with patients with macroscopic residual disease.<sup>6,8,9</sup> Thus, clear tumor visualization is pivotal for optimal staging and macroscopical radical resection; as Sugarbaker himself stressed, "It's what the surgeon doesn't see that kills the patient."<sup>10</sup> At present, surgeons must rely on inspection with the naked eye and palpation for intraoperative tumor detection.

Near-infrared (NIR: 700–900 nm) fluorescence imaging is a relatively novel imaging modality. This technique is eminently suitable for real-time intraoperative application as the NIR fluorescent signal can be acquired within milliseconds. Moreover, NIR fluorescent light is invisible to the human eye and therefore does not permanently alter the surgical field and can travel up to 1 cm through tissue allowing signal detection



below the tissue surface.<sup>11–13</sup> Near-infrared fluorescence imaging can make use of endogenous tissue properties, but more commonly, an exogenous fluorescent contrast agent is administered intravenously. These fluorescent contrast agents can be coupled with targeting moieties that specifically bind to a target, ie, tumor protein. Using an open or laparoscopic NIR fluorescence imaging device, the target can be detected by the fluorescent signal arising from the contrast agent.<sup>14</sup> The enhanced contrast between cancerous and benign tissue will enable the surgeon to clearly visualize tumor lesions in real-time during surgery. In the case of CRS, this will greatly aid in the initial assessment of PM extent but will also potentially allow an increase in macroscopically radical resections. The first clinical trials with tumor-specific fluorescent contrast agents report successful intraoperative fluorescence imaging of malignant glioma, head and neck, ovarian, and lung cancers.<sup>15–19</sup> Studies with patients with ovarian cancer are especially interesting, as in this cancer type PM is also frequently seen. Both studies demonstrated that it was possible to visualize PM in ovarian cancer using a folate receptor–targeting fluorescent agent.<sup>16,19</sup> Fluorescence imaging led to the detection and subsequent resection of additional tumor lesions that were otherwise not detected.

These results encourage investigation of fluorescence imaging in PM of CRC. Selection of tumor-targeting fluorescent contrast agents suitable for imaging of PM of CRC requires identification of biomarkers with overexpression on PM of CRC. Immunohistochemical (IHC) staining of tumor tissue is a validated and commonly used technique to assess the degree of expression levels of specific biomarkers. The aim of this study is to assess the suitability of various biomarkers for tumor-targeted fluorescence imaging of PM of CRC using IHC. Upregulation of numerous biomarkers in colorectal tumor tissues is described in the literature.<sup>20</sup> Our selection of biomarkers is based on the availability of fluorescence agents and the Target Selection Criteria (TASC) scoring system for biomarkers for imaging purposes.<sup>21</sup> When expression of a biomarker on a PM is concordant with expression on the primary tumor, staining of the primary tumor could predict PM expression and aid in patient selection. Therefore, we also aimed to determine the concordance between biomarker expression on the primary tumor and the corresponding PM.

## Methods

### *Sample selection*

Tissue samples of all patients diagnosed with CRC who underwent CRS and HIPEC procedure in Erasmus Medical Center between March 2014 and September 2015 (n=36) were reviewed. Formalin-fixed, paraffin-embedded (FFPE) tissue blocks were obtained from the pathology archives of the Erasmus Medical Center and the primary care facility if the primary tumor was previously resected elsewhere. This study was approved by the Institutional Ethics Committee of the

Leiden University Medical Center (LUMC). All samples were handled anonymously and used in accordance with the ethical standards of the local ethics committee and with national Dutch guidelines (“Code for Proper Secondary Use of Human Tissues,” Dutch Federation of Medical Scientific Societies).

### *Immunohistochemistry*

Sections of 4 μm were sliced, collected on StarFrost adhesive slides, and dried overnight. Sections were deparaffinized in a series of xylene and rehydrated in decreasing concentrations of ethanol. After rinsing in distilled water, slides were incubated in 0.3% H<sub>2</sub>O<sub>2</sub> for 20 minutes to block endogenous peroxidase, followed by a washing step in water. Antigen retrieval was performed in EnVision FLEX Target Retrieval Solution, Low pH (PT Link; Dako, Santa Clara, CA, USA) for 10 minutes at 95°C.

Antibodies used for IHC staining of carcinoembryonic antigen (CEA), tyrosine-protein kinase Met (C-Met), epithelial cell adhesion molecule (EpCAM), and folate receptor α (FRα) were as follows: monoclonal mouse anti-CEACAM5, Clone CI-P83-1 (sc-23928; 0.5 μg/mL; Santa Cruz, Dallas, TX, USA), polyclonal rabbit anti-cMet (sc-10; 0.5 μg/mL; Santa Cruz), monoclonal anti-EpCAM, clone MOC31 (DM2014A; 0.05 μg/mL; Acris Antibodies, Herford, Germany), and monoclonal mouse anti-FRα, clone 26B3.F2 (IHC Assay Kit; 4006 K; Biocare Medical, Pacheco, CA, USA). Folate receptor α staining was done following manufacturer’s instructions. Normal lung tissue was included as positive control for FRα staining; for the other 3 biomarkers, an internal positive control was present. For CEA, C-Met, and EpCAM staining, primary antibodies were incubated overnight at room temperature, followed by 3 washes with phosphate-buffered saline and incubation with EnVision anti-mouse-HRP or EnVision anti-rabbit-HRP (Dako) for 30 minutes at room temperature. After another 3 washes, antibody binding was visualized using 3,3′-diaminobenzidine for 5 minutes. Sections were rinsed in deionized water, counterstained with hematoxylin, dehydrated, and mounted with Pertex. Next to immunohistochemistry, hematoxylin and eosin staining was performed for routine pathological evaluation. All slides were scanned using the Ultra Fast Scanner (Philips, Eindhoven, The Netherlands).

### *Scoring method*

Biomarker expression for the different biomarkers was assessed in both primary tumor and PM tissue using an intensity scoring method with a scale ranging from 0 to 3+ (0 for absence of staining, 1+ for weak staining, 2+ for moderate staining, and 3+ for strong staining). This score was applied to the epithelial and stromal staining. Representative images of these intensity scores are depicted in Figure 1. When various tumor cells within a tumor exhibited different intensity scores (eg, both 1+ and 2+), the highest score was noted. In addition to the intensity, also the percentage of positive staining tumor

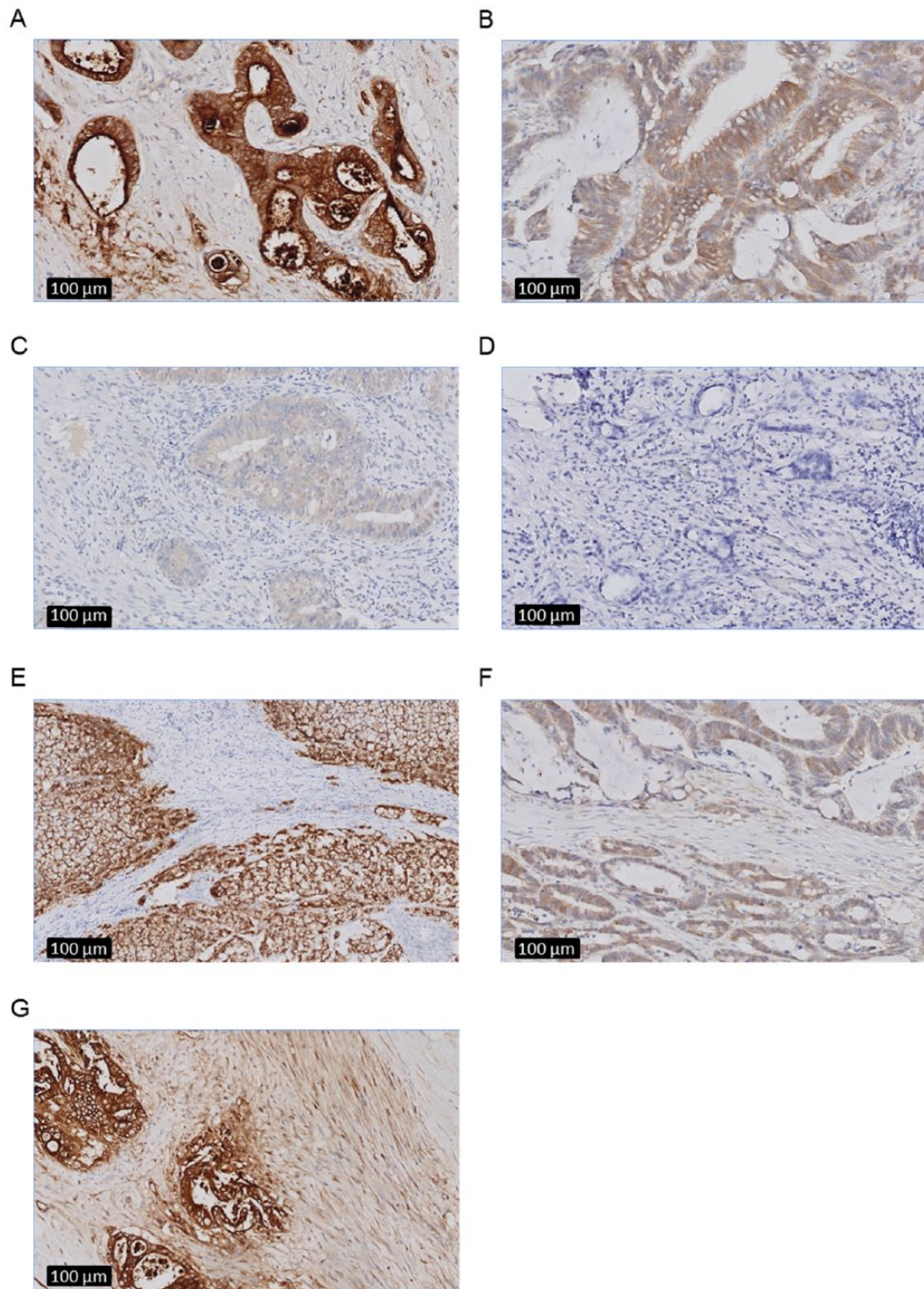


**Figure 1.** Representative epithelial and stromal staining intensities in peritoneal metastasis from colorectal cancer using immunohistochemistry (as specified in the Methods section) at zoom 10x after immunohistochemistry. Examples of (A) strong 3+ epithelial staining intensity (CEA), (B) moderate 2+ epithelial staining intensity (C-Met), (C) weak 1+ epithelial staining intensity (C-Met), (D) absent 0 epithelial staining (FR $\alpha$ ), (E) absent 0 stromal staining (EpCAM), (F) weak 1+ stromal staining (C-Met), and (G) moderate 2+ stromal staining (CEA). CEA indicates carcinoembryonic antigen; FR $\alpha$ , folate receptor  $\alpha$ .

cells was assessed. Percentages were recorded in quartiles (25%, 50%, 75%, and 100%). For the purpose of this study, the intensity scores and percentages were combined in a final expression score, calculated using the following formula:

Expression score = (Intensity score - 1) \* 4 + (Percentage of observed expression / 25). This gives a linear score of 0 to 12, with a score of 0 corresponding to absent expression and a score of 12 corresponding to strong (3+) intensity expression

in 100% of tumor cells.<sup>22</sup> The tumor was considered positive, and thus, the biomarker suitable for intraoperative fluorescence imaging when the expression score of tumor cells or tumor stroma was  $\geq 5$ . Strong overexpression was defined as a combined score  $\geq 9$ , indicating an expression pattern highly suitable for tumor imaging.

Concordance was established when the expression score of the primary tumor matched the expression score of the PM. Evaluation of the IHC staining was performed blinded and independently by 2 observers. In case of disagreements, the staining was discussed to reach consensus among the observers. If still no agreement was reached, the relevant staining was evaluated with a third observer, specialized in CRC pathology.

### Statistical analysis

All statistical analyses were performed using the SPSS (version 23; IBM, Chicago, IL, USA) and GraphPad Prism 6 (GraphPad Software Inc., La Jolla, CA, USA). Statistical evaluation of inter-rater reliability was not performed. The correlation between primary tumor and PM was calculated using the Spearman correlation coefficient ( $\rho$ ). Perfect correlation was considered as Spearman correlation coefficient of 1 or -1. Spearman correlation coefficient values close to or  $<0$  were considered as poor correlation. *P* value of  $<.05$  was considered statistically significant.

### Results

Incomplete sets of primary tumor and PM, as a result of inability to obtain a primary tumor sample from another hospital ( $n=5$ ) or absence of PM in pathology samples ( $n=8$ ), were discarded from further analysis. A total of 23 sets were included in the staining protocol. During the staining procedure, the sets containing an empty or broken FFPE block ( $n=3$ ) were excluded, resulting in a total of 20 sets for the final analysis. Histology of primary tumors was mostly adenocarcinoma (16/20) and mucinous adenocarcinoma in the remaining samples (4/20). For the primary tumor, 20 samples (100%) demonstrated expression of both EpCAM and CEA. Strong expression was seen in almost all cases (95%) for EpCAM and to a lesser extent for CEA (70%). The C-Met and FR $\alpha$  expression was positive in a smaller part of primary tumor samples, 15% and 30%, respectively. Strong expression was not seen for C-Met and only in 1 sample (5%) for FR $\alpha$ . Stromal expression was only seen in samples stained for CEA, with a positive expression in about half of the samples (45%). For EpCAM and FR $\alpha$ , stromal staining was absent, and for C-Met, stromal staining was seen in most samples (75%), but expression was too low ( $<5$ ) to qualify the staining as positive (Table 1).

For the PM, 20 samples (100%) demonstrated epithelial expression of EpCAM and CEA staining. The staining was strong in 90% of samples for EpCAM and in 70% of samples for CEA. These percentages are similar to the percentages of the primary tumor. Stromal staining was not seen for EpCAM;

**Table 1.** Biomarker expression in primary colorectal tumors and corresponding peritoneal metastasis.

|                                | EPICAM               |                                  | CEA                  |                                  | C-MET                |                                  | FR $\alpha$          |                                  |
|--------------------------------|----------------------|----------------------------------|----------------------|----------------------------------|----------------------|----------------------------------|----------------------|----------------------------------|
|                                | PRIMARY TUMOR (N=20) | PERITONEAL CARCINOMATOSIS (N=20) | PRIMARY TUMOR (N=20) | PERITONEAL CARCINOMATOSIS (N=20) | PRIMARY TUMOR (N=20) | PERITONEAL CARCINOMATOSIS (N=20) | PRIMARY TUMOR (N=20) | PERITONEAL CARCINOMATOSIS (N=20) |
|                                | NO. (%)              | NO. (%)                          | NO. (%)              | NO. (%)                          | NO. (%)              | NO. (%)                          | NO. (%)              | NO. (%)                          |
| Positive epithelial expression | 20 (100)             | 20 (100)                         | 20 (100)             | 20 (100)                         | 3 (15)               | 4 (20)                           | 6 (30)               | 4 (20)                           |
| Strong epithelial expression   | 19 (95)              | 18 (90)                          | 14 (70)              | 14 (70)                          | 0 (0)                | 0 (0)                            | 1 (5)                | 0 (0)                            |
| Positive stromal expression    | 0 (0)                | 0 (0)                            | 9 (45)               | 9 (45)                           | 0 (0)                | 1 (5)                            | 0 (0)                | 0 (0)                            |
| Strong stromal expression      | 0 (0)                | 0 (0)                            | 0 (0)                | 0 (0)                            | 0 (0)                | 0 (0)                            | 0 (0)                | 0 (0)                            |
| Total positive expression      | 20 (100)             | 20 (100)                         | 20 (100)             | 20 (100)                         | 3 (15)               | 5 (25)                           | 6 (30)               | 4 (20)                           |
| Total strong expression        | 19 (95)              | 18 (90)                          | 14 (70)              | 14 (70)                          | 0 (0)                | 0 (0)                            | 1 (5)                | 0 (0)                            |

Abbreviations: CEA, carcinoembryogenic antigen; EpCAM, epithelial cell adhesion molecule; FR $\alpha$ , folate receptor  $\alpha$ .

however, stromal CEA expression was again noted in 45% of samples. Five PM samples had a positive expression for C-Met (25%), including 4 tissues with positive epithelial expression and 1 tissue with stromal expression. The FR $\alpha$  expression was slightly lower, 20%, and limited to epithelial expression. Strong C-Met or FR $\alpha$  expression was not seen in any of the PM samples (Table 1).

Concordance between expression scores of primary tumor and PM was assessed using the Spearman correlation coefficient. A significant moderate to strong correlation between primary tumor and PM was seen for the EpCAM (0.688) and FR $\alpha$  (0.803) epithelial expression score and for the C-Met (0.461) stromal expression score. For all other scores, correlation between primary tumor and PM was weak (<0.39). When comparing both the mean tumor and PM score (Table 2), a clear compatibility is seen between the primary tumor and PM expression score.

**Discussion**

Clear intraoperative tumor visualization using NIR fluorescence imaging could improve both diagnosis and treatment of patients with PM of CRC. Near-infrared fluorescence imaging can be performed during open as well as laparoscopic surgery and can be applied to various oncologic surgeries, making the technique suitable for all centers performing colorectal surgeries. Potential benefits of fluorescence imaging are already reported in patients with PM from ovarian cancer using an ovarian cancer-specific agent.<sup>16,19</sup> Extrapolation of these results to patients with CRC requires identification of tumor targets with overexpression on PM of CRC.

Upregulation of numerous biomarkers in CRC is described in the literature.<sup>20</sup> Suitability of a certain biomarker for fluorescence imaging is not only determined by its upregulation but also influenced by various other factors. In general, an optimal target exhibits strong and homogeneous overexpression in most of the tumors. In an attempt to objectively assess the suitability of a potential biomarker for tumor targeting, Oosten et al<sup>21</sup> proposed the use of the TASC scoring system. In addition to the previously mentioned factors, this system gives scores for extracellular localization of the biomarker, previous use of the biomarker in in vivo imaging studies, enzymatic activity in or around tumor tissue (which will allow the use of activatable agents), and internalization of the agent. This adds up to a maximum score of 22 points. A biomarker with a score  $\geq 18$  should be considered as a potential target. When applying this score to biomarkers for CRC, 6 potential targets, including CEA, EpCAM, and FR $\alpha$ , for tumor-targeted imaging are identified.<sup>23</sup> The clinical evaluation and use of these potential targets is entirely depending on the availability of imaging agents for these targets. Folate receptor  $\alpha$  and C-Met targeting clinical agents have been studied in small groups of patients, and properties of these agents were found to be suitable for fluorescence imaging.<sup>16,19,24</sup> A fluorescent agent targeting EpCAM is expected to reach the clinic by the end of this year and a

**Table 2.** Mean biomarker expression scores for primary colorectal tumors and corresponding peritoneal metastasis and their correlation using Spearman correlation coefficient.

|                             | EPCAM                |                                  |                         | CEA                  |                                  |                         | C-MET                |                                  |                         | FR $\alpha$          |                                  |                         |
|-----------------------------|----------------------|----------------------------------|-------------------------|----------------------|----------------------------------|-------------------------|----------------------|----------------------------------|-------------------------|----------------------|----------------------------------|-------------------------|
|                             | PRIMARY TUMOR (N=20) | PERITONEAL CARCINOMATOSIS (N=20) | CORRELATION COEFFICIENT | PRIMARY TUMOR (N=20) | PERITONEAL CARCINOMATOSIS (N=20) | CORRELATION COEFFICIENT | PRIMARY TUMOR (N=20) | PERITONEAL CARCINOMATOSIS (N=20) | CORRELATION COEFFICIENT | PRIMARY TUMOR (N=20) | PERITONEAL CARCINOMATOSIS (N=20) | CORRELATION COEFFICIENT |
| Epithelial expression score | 11.8 (0.9)           | 11.6 (1.2)                       | 0.688                   | 10.6 (2.0)           | 10.6 (2.1)                       | 0.128                   | 3.9 (1.8)            | 4.1 (2.2)                        | -0.024                  | 2.2 (3.0)            | 1.6 (2.3)                        | 0.803                   |
| Stromal expression score    | 0.1 (0.3)            | 0.1 (0.2)                        | -0.076                  | 3.1 (2.4)            | 3.1 (2.9)                        | 0.191                   | 1.8 (1.5)            | 2.3 (1.6)                        | 0.461                   | 0.0 (0.0)            | 0.1 (0.2)                        | NA                      |

Abbreviations: CEA, carcinoembryonic antigen; EpCAM, epithelial cell adhesion molecule; FR $\alpha$ , folate receptor  $\alpha$ ; NA, not applicable.

fluorescent-labeled anti-CEA antibody is currently studied in patients with CRC (NTR5673). In this study, we evaluated the most eligible targets for clinical imaging of CRC. The most frequently expressed biomarkers on PM were EpCAM and CEA. Positive epithelial expression for these biomarkers was seen in all samples, and most of the samples showed strong expression. Expression of C-Met and FR $\alpha$  was seen in only 1 out of 5 PM samples and expression was never strong. Therefore, from the evaluated markers, EpCAM seems the most favorable target for intraoperative fluorescence imaging of PM. For CEA, a similar expression pattern is found, although a strong expression is seen less frequent compared with EpCAM. A potential advantage of CEA as imaging target is that apart from expression on the epithelium, CEA is also expressed in the stroma surrounding tumor cells. Stroma is often abundantly present in aggressive tumors and is located at the border, at the invasive front of the tumor, a location particularly suited for NIR fluorescence imaging.<sup>25</sup> From our data, C-Met and FR $\alpha$  seem less favorable targets, as expression was not consistently seen in PM and the level of expression was never strong. Folate receptor  $\alpha$  expression of the primary tumor did show a significant and strong correlation with the expression of the PM; therefore, staining of the primary tumor to predict presence of positive expression in the PM is feasible. Weak correlation coefficients between expression of the primary tumor and PM were seen for most other biomarkers; this is likely a consequence of the small variability between scores, which causes a high likelihood that the same scores are given based on chance. We expect that tumor heterogeneity will have an impact on this technique. However, due to the retrospective nature of this study our sample selection was limited to 1 PM sample per patient, which precludes assessment of the effect of tumor heterogeneity.

The biomarkers evaluated in this study are suitable for tumor-targeted fluorescence imaging. Two recently published studies describe fluorescence-guided surgery of PM in patients with CRC using the nontargeted dye indocyanine green (ICG).<sup>26,27</sup> As ICG does not specifically target tumor biomarkers, the use of ICG for fluorescence imaging is based on processes that cause aspecific accumulation of the agent in or around the tumor. Liberale et al<sup>26</sup> hypothesize that if it is possible to visualize small liver tumors or colorectal liver metastases using ICG, it will also be possible to visualize PM from CRC. However, retention of ICG around liver tumors is largely a consequence of the hepatic clearance of ICG.<sup>28,29</sup> As this process does not apply to PM, accumulation of ICG in PM was likely the result of the increased vascular permeability and reduced drainage in tumor tissue following tumor-induced angiogenesis (the enhanced permeability and retention [EPR] effect).<sup>30,31</sup> It is very likely that the lack of specificity of the EPR effect precludes successful application for intraoperative imaging.<sup>32</sup> Moreover, detection of small PM lesions (<2 mm) based on the EPR effect is most likely not possible as these lesions are still avascular, eg, before the angiogenic switch.<sup>33</sup> Therefore, the need for tumor-specific fluorescent agents remains.

We are aware that our study contains several limitations. First, selection of the biomarkers was not fully comprehensive because the selection was also based on availability of fluorescence imaging agents for these biomarkers. Second, the analyzed sample size is relatively small. Nevertheless, the study represents the largest cohort of patients with CRC investigated for fluorescence imaging of PM. And, third, IHC staining was not performed on adjacent normal colon tissue. For successful image-guided surgery, it is essential that the fluorescence ratio between tumor tissue and healthy background tissue (tumor-to-background ratio) is greater than 2.<sup>11</sup> The fluorescence ratio is determined by various factors including affinity of the fluorescent agent for the biomarker, clearance from normal tissues, and upregulation of biomarker on cancer cells. Concerning upregulation of the biomarker, a tumor-to-normal (T/N) ratio of greater than 10 is generally considered sufficient.<sup>34</sup> Although not specifically addressed in this study, expression of EpCAM, CEA, C-Met, and FR $\alpha$  on normal tissue is well described in the literature, and all mentioned biomarkers apart from C-Met have a T/N ratio >10. For C-Met variable, T/N ratios were reported, ranging from 0.2 to 50.<sup>35,36</sup> Equally important is the expression on abnormal, nonmalignant tissue, ie, scar tissue or inflamed tissue. This should be assessed, as absent or low expression is warranted to prevent false positive fluorescence. Although false-positive fluorescence is undesirable, it is not unsurmountable as long as the sensitivity is high, eg, missing malignant lesions have worse implications than resection of nonmalignant lesions. Finally, the effect of various neoadjuvant treatments on biomarker upregulation in remaining vital tumor cells should be studied.

## Conclusions

In conclusion, this study provides valuable insights in the optimal target for intraoperative fluorescence imaging of PM from CRC. Positive and generally strong expression of both EpCAM and CEA was found on PM samples, making these biomarkers pre-eminently suitable for fluorescence detection of PM from patients with CRC undergoing CRS and HIPEC. A fluorescent agent targeting EpCAM is expected to reach the clinic by the end of this year, and a fluorescent-labeled anti-CEA antibody is currently studied in patients with CRC (NTR5673). Therefore, the first intraoperative fluorescence imaging trials in PM from CRC using tumor-targeting agents could be approaching soon.

## Acknowledgements

The authors thank Arvind Oemrawsingh and the Erasmus MC Pathology Department for their assistance in assembling the FFPE tissue blocks and Tom van Ravens for his assistance in sectioning of the FFPE tissue blocks.

## Author Contributions

CH, BW, LB, JB, CV, AFS, JB, and AV conceived and designed the experiments. CH, BW, LB, DH, HP, CS, SB, AFS, JB, and

AV analyzed the data. CH, BW, and CS wrote the first draft of the manuscript. LB, HP, CS, JB, CV, SB, AFS, JB, and AV contributed to the writing of the manuscript. CH, BW, LB, JB, CV, DH, HP, CS, SB, AFS, JB, and AV agree with manuscript results and conclusions. CH, BW, LB, JB, CV, DH, HP, CS, SB, AFS, JB, and AV jointly developed the structure and arguments for the paper. LB, HP, CS, JB, CV, SB, AFS, JB, and AV made critical revisions and approved final version. All authors reviewed and approved the final manuscript.

## REFERENCES

- Thomassen I, Van Gestel YR, Lemmens VE, De Hingh IH. Incidence, prognosis, and treatment options for patients with synchronous peritoneal metastasis and liver metastases from colorectal origin. *Dis Colon Rectum*. 2013;56:1373–1380.
- Sugarbaker PH, Zhu BW, Sese GB, Shmookler B. Peritoneal metastasis from appendiceal cancer: results in 69 patients treated by cytoreductive surgery and intraperitoneal chemotherapy. *Dis Colon Rectum*. 1993;36:323–329.
- Esquivel J, Chua TC. CT versus intraoperative peritoneal cancer index in colorectal cancer peritoneal metastasis: importance of the difference between statistical significance and clinical relevance. *Ann Surg Oncol*. 2009;16:2662–2663; author reply 2264.
- Koh JL, Yan TD, Glenn D, Morris DL. Evaluation of preoperative computed tomography in estimating peritoneal cancer index in colorectal peritoneal metastasis. *Ann Surg Oncol*. 2009;16:327–333.
- Verwaal VJ, Van Ruth S, De Bree E, et al. Randomized trial of cytoreduction and hyperthermic intraperitoneal chemotherapy versus systemic chemotherapy and palliative surgery in patients with peritoneal metastasis of colorectal cancer. *J Clin Oncol*. 2003;21:3737–3743.
- Shen P, Levine EA, Hall J, et al. Factors predicting survival after intraperitoneal hyperthermic chemotherapy with mitomycin C after cytoreductive surgery for patients with peritoneal metastasis. *Arch Surg*. 2003;138:26–33.
- Goere D, Souadka A, Faron M, et al. Extent of colorectal peritoneal carcinomatosis: attempt to define a threshold above which HIPEC does not offer survival benefit: a comparative study. *Ann Surg Oncol*. 2015;22:2958–2964.
- Sugarbaker PH, Chang D, Koslowe P. Prognostic features for peritoneal metastasis in colorectal and appendiceal cancer patients when treated by cytoreductive surgery and intraperitoneal chemotherapy. *Cancer Treat Res*. 1996;81:89–104.
- Elias D, Quenet F, Goere D. Current status and future directions in the treatment of peritoneal dissemination from colorectal carcinoma. *Surg Oncol Clin N Am*. 2012;21:611–623.
- Sugarbaker PH. It's what the surgeon doesn't see that kills the patient. *J Nippon Med Sch*. 2000;67:5–8.
- Vahrmeijer AL, Hutteman M, Van der Vorst JR, Van de Velde CJ, Frangioni JV. Image-guided cancer surgery using near-infrared fluorescence. *Nat Rev Clin Oncol*. 2013;10(9):507–518.
- Chance B. Near-infrared images using continuous, phase-modulated, and pulsed light with quantitation of blood and blood oxygenation. *Ann N Y Acad Sci*. 1998;838:29–45.
- Frangioni JV. In vivo near-infrared fluorescence imaging. *Curr Opin Chem Biol*. 2003;7:626–634.
- Keereweer S, Kerrebijn JD, Van Driel PB, et al. Optical image-guided surgery—where do we stand? *Mol Imaging Biol*. 2011;13:199–207.
- Stummer W, Stocker S, Wagner S, et al. Intraoperative detection of malignant gliomas by 5-aminolevulinic acid-induced porphyrin fluorescence. *Neurosurgery*. 1998;42(3):518–525; discussion 525–516.
- Van Dam GM, Themelis G, Crane LM, et al. Intraoperative tumor-specific fluorescence imaging in ovarian cancer by folate receptor- $\alpha$  targeting: first in-human results. *Nat Med*. 2011;17:1315–1319.
- Kennedy GT, Okusanya OT, Keating JJ, et al. The optical biopsy: a novel technique for rapid intraoperative diagnosis of primary pulmonary adenocarcinomas. *Ann Surg*. 2015;262(4):602–609.
- Rosenthal EL, Warram JM, De Boer E, et al. Safety and tumor specificity of cetuximab-IRDye800 for surgical navigation in head and neck cancer. *Clin Cancer Res*. 2015;21:3658–3666.
- Hoogstins CE, Tummers QR, Gaarenstroom KN, et al. A novel tumor-specific agent for intraoperative near-infrared fluorescence imaging: a translational study in healthy volunteers and patients with ovarian cancer. *Clin Cancer Res*. 2016;22:2929–2938.
- Cardoso J, Boer J, Morreau H, Fodde R. Expression and genomic profiling of colorectal cancer. *Biochim Biophys Acta*. 2007;1775:103–137.
- Van Oosten M, Crane LM, Bart J, Van Leeuwen FW, Van Dam GM. Selecting potential targetable biomarkers for imaging purposes in colorectal cancer using TArget Selection Criteria (TASC): a novel target identification tool. *Transl Oncol*. 2011;4:71–82.
- Ren J, Chen QC, Jin F, et al. Overexpression of Rsf-1 correlates with pathological type, p53 status and survival in primary breast cancer. *Int J Clin Exp Pathol*. 2014;7:5595–5608.
- Hutteman M, Mieog JS, Van der Vorst JR, et al. Intraoperative near-infrared fluorescence imaging of colorectal metastases targeting integrin  $\alpha(v)\beta(3)$  expression in a syngeneic rat model. *Eur J Surg Oncol*. 2011;37:252–257.
- Burggraaf J, Kamerling IM, Gordon PB, et al. Detection of colorectal polyps in humans using an intravenously administered fluorescent peptide targeted against c-Met. *Nat Med*. 2015;21:955–961.
- Boonstra MC, Prakash J, Van De Velde CJ, et al. Stromal targets for fluorescent-guided oncologic surgery. *Front Oncol*. 2015;5:254.
- Liberalo G, Vankerckhove S, Caldon MG, et al. Fluorescence imaging after indocyanine green injection for detection of peritoneal metastases in patients undergoing cytoreductive surgery for peritoneal metastasis from colorectal cancer: a pilot study. *Ann Surg*. 2016;264:1110–1115.
- Filippello A, Porcheron J, Klein JP, Cottier M, Barabino G. Affinity of indocyanine green in the detection of colorectal peritoneal metastasis. *Surg Innov*. 2017;24:103–108.
- Van der Vorst JR, Schaafsma BE, Hutteman M, et al. Near-infrared fluorescence-guided resection of colorectal liver metastases. *Cancer*. 2013;119:3411–3418.
- De Graaf W, Hausler S, Heger M, et al. Transporters involved in the hepatic uptake of (99m)Tc-mebrofenin and indocyanine green. *J Hepatol*. 2011;54:738–745.
- Maeda H, Wu J, Sawa T, Matsumura Y, Hori K. Tumor vascular permeability and the EPR effect in macromolecular therapeutics: a review. *J Control Release*. 2000;65:271–284.
- Matsumura Y, Maeda H. A new concept for macromolecular therapeutics in cancer chemotherapy: mechanism of tumorotropic accumulation of proteins and the antitumor agent smancs. *Cancer Res*. 1986;46:6387–6392.
- Tummers QR, Hoogstins CE, Peters AA, et al. The value of intraoperative near-infrared fluorescence imaging based on enhanced permeability and retention of indocyanine green: feasibility and false-positives in ovarian cancer. *PLoS ONE*. 2015;10:e0129766.
- Bergers G, Benjamin LE. Tumorigenesis and the angiogenic switch. *Nat Rev Cancer*. 2003;3:401–410.
- Sega EI, Low PS. Tumor detection using folate receptor-targeted imaging agents. *Cancer Metastasis Rev*. 2008;27:655–664.
- Di Renzo MF, Olivero M, Giacomini A, et al. Overexpression and amplification of the met/HGF receptor gene during the progression of colorectal cancer. *Clin Cancer Res*. 1995;1:147–154.
- Prat M, Narsimhan RP, Crepaldi T, Nicotra MR, Natali PG, Comoglio PC. The receptor encoded by the human c-MET oncogene is expressed in hepatocytes, epithelial cells and solid tumors. *Int J Cancer*. 1991;49:323–328.